Terahertz pulsed spectroscopic imaging using optimized binary masks

Y. C. Shen,[1,a)] L. Gan,[2] M. Stringer,[3] A. Burnett,[3] K. Tych,[3] H. Shen,[1] J. E. Cunningham,[3] E. P. J. Parrott,[4] J. A. Zeitler,[4] L. F. Gladden,[4] E. H. Linfield,[3] and A. G. Davies[3]
[1]*Department of Electrical Engineering and Electronics, University of Liverpool, Liverpool L69 3GJ, United Kingdom*
[2]*Electronic and Computer Engineering, School of Engineering and Design, Brunel University, Uxbridge UB8 3PH, United Kingdom*
[3]*School of Electronic and Electrical Engineering, University of Leeds, Leeds LS2 9JT, United Kingdom*
[4]*Department of Chemical Engineering and Biotechnology, University of Cambridge, Cambridge CB2 3RA, United Kingdom*

(Received 5 October 2009; accepted 8 November 2009; published online 10 December 2009)

We report the development of a terahertz pulsed spectroscopic imaging system based on the concept of compressive sensing. A single-point terahertz detector, together with a set of 40 optimized two-dimensional binary masks, was used to measure the terahertz waveforms transmitted through a sample. Terahertz time- and frequency-domain images of the sample comprising 20×20 pixels were subsequently reconstructed. We demonstrate that both the spatial distribution and the spectral characteristics of a sample can be obtained by this means. Compared with conventional terahertz pulsed imaging, no raster scanning of the object is required, and ten times fewer terahertz spectra need be taken. It is therefore ideal for real-time imaging applications. © *2009 American Institute of Physics*. [doi:10.1063/1.3271030]

The terahertz frequency region of the electromagnetic spectrum (0.3–10 THz, 10–330 cm^{-1}) offers a unique combination of properties. Many crystalline substances possess sharp characteristic spectral features in this frequency range associated with both inter- and intramolecular vibrational modes.[1,2] This, when coupled with the ability of terahertz radiation to propagate through common barrier materials, such as clothing and packaging, makes terahertz imaging and spectroscopy a potentially powerful tool for nondestructive determination of the chemical composition and physical structure of a concealed sample.[3] Indeed, over the past decade, terahertz time-domain (pulsed) imaging has been demonstrated in applications areas as diverse as the medical diagnosis of human tissue, the detection and chemical mapping of illicit drugs and explosives, and pharmaceutical tablet inspection.[4–7]

However, because of the relatively modest power levels available from the photoconductive sources commonly used in terahertz time-domain spectroscopy and imaging systems, and the lack of compact and sensitive multi-element terahertz detectors, most terahertz pulsed imaging experiments have been performed by raster scanning the object relative to a focused terahertz beam, and by using a single-point detector. Consequently, a complete image usually takes minutes or even hours to acquire, depending on the total number of pixels and the required spectral range/resolution. This is a major limiting factor for real-time applications such as *in vivo* medical and security imaging, or for on-line industrial process monitoring.

Recently Chan *et al.*[8,9] reported a new terahertz imaging procedure, based on compressive sampling.[10] The free-space pulsed terahertz wave front traveling from an object to a single-point detector was spatially modulated by the insertion of a series of planar two-dimensional (2D) masks. Each mask comprised a random checkerboard pattern of 32 $\times32$ pixels that could each either transmit or block the terahertz radiation. By recording the terahertz field in the presence of each mask, a 2D image of the object was reconstructed.[8] This approach not only eliminates the need to raster scan the object or terahertz beam, but also reduces the number of measurements required.[8] This is a significant improvement in speed compared with the traditional raster scanning used for terahertz imaging (assuming that the masks can be changed automatically, for example, by using the newly developed terahertz spatial modulator[11]). In this letter, we report that pulsed terahertz *spectroscopic* imaging is possible using a single-point detector and compressive sampling, allowing both a spatial and chemical map of a sample to be obtained.

Figure 1 shows our experimental arrangement, which is similar to that typically used for the coherent generation and detection of broadband terahertz radiation.[12] A Ti:sapphire laser provides visible/near-infrared pulses of 12 fs duration at a center wavelength of 790 nm with a repetition rate of 76 MHz. The output is split into two parts: a 330 mW beam

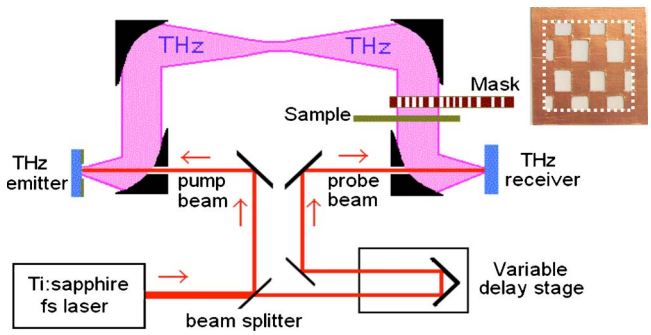

FIG. 1. (Color online) Experimental arrangement for terahertz pulsed imaging using compressive sampling. The inset shows one of 40 masks with the dotted line indicating the 40×40 mm^2 imaging area. The copper pixels are opaque to terahertz radiation while the white pixels are transparent to terahertz radiation.

a)Electronic mail: y.c.shen@liverpool.ac.uk.

is used for terahertz generation and a 40 mW beam serves as the probe beam for terahertz detection. Terahertz radiation is generated from a low-temperature-grown GaAs photoconductive emitter with an electrode gap of 0.4 mm and is biased using a 10 kHz square wave of peak amplitude ± 100 V. The terahertz pulses emitted (in the "reflection" geometry[12]) are collimated and focused onto a 1-mm-thick (110) ZnTe crystal for electro-optic detection. Only one pair of parabolic mirrors is required for imaging using the compressive sampling technique as the sample (and the binary masks) is placed in a collimated terahertz beam. In our experimental arrangement, however, we retained two pairs of parabolic mirrors to allow conventional terahertz time-domain pulsed spectroscopy measurements to allow, in addition, conventional terahertz time-domain pulsed spectroscopy measurement to be performed.

Consider an $I_r \times I_c$ image, with $N=I_rI_c$ pixels in total, and suppose that one wants to sample it using only $M(<N)$ measurements. Let x denote the vector signal of the N-pixel input image. The measurement process can be described as $\mathbf{y}=\Phi\mathbf{x}$, where $\mathbf{y}$ is an $M\times 1$ measured vector and Φ is an $M\times N$ binary matrix, whose ith $(1\leq i\leq M)$ row corresponds to the ith measurement. The selection of the measurement operator Φ holds the key to the quality of the reconstructed image. Typically, a set of random measurement functions/masks are used in compressive sampling,[8,10] which can provide many advantages, such as universality, weak encryption, and robustness to channel losses. However, it has been noted that random projections do not work well at low signal-to-noise ratios or at low sampling rates.[13,14] Here we used an optimized mask set, aiming to reduce further the number of necessary measurements, while still retaining the quality of the reconstructed image. In brief, the binary masks are optimized to approximate the Karhunen–Loeve transform (KLT). The idea is quite similar to that of Ref. 15 where the 2D discrete cosine transform is quantized with the ternary set $\{1,0,-1\}$. Specifically, we assume that the autocorrelation matrix $\mathbf{R}_{xx}$ of the input image follows the isotropic 2D model with correlation coefficient 0.95.[16] The $M\times N$ floating-coefficient KLT matrix $\mathbf{U}$ is then obtained through the eigenvalue decomposition of $\mathbf{R}_{xx}$. After that, we use MATLAB 7.0 to search an optimal threshold T so that the binary matrix $\Phi(k,l)$ defined below yields the maximum coding gain,[16]

$$\Phi(k,l)=\begin{cases}1, & \mathbf{U}(k,l)>T,\\ 0, & \text{otherwise}.\end{cases}$$

The binary matrix $\Phi(k,l)$ is then used to make the masks. The inset to Fig. 1 shows one of the 40 masks used. Our masks each comprised 20×20 pixels and were constructed from self-supported copper tape. Each pixel had dimensions of 2×2 mm^2, thus providing a 40×40 mm^2 imaging area. It was confirmed that the pixels were either totally transparent or totally opaque to terahertz radiation. The lack of a supporting substrate eliminates possible terahertz absorption/dispersion or phase delays in propagation through the transparent pixels, making this design ideal for broadband spectroscopic imaging applications.

A sample comprising regions of polyethylene, lactose, and copper tape (Fig. 2 inset) was placed in the collimated terahertz beam path together with one of the 40 masks, and the terahertz electric field was recorded as a function of time delay using the time-domain spectroscopy system. In total,

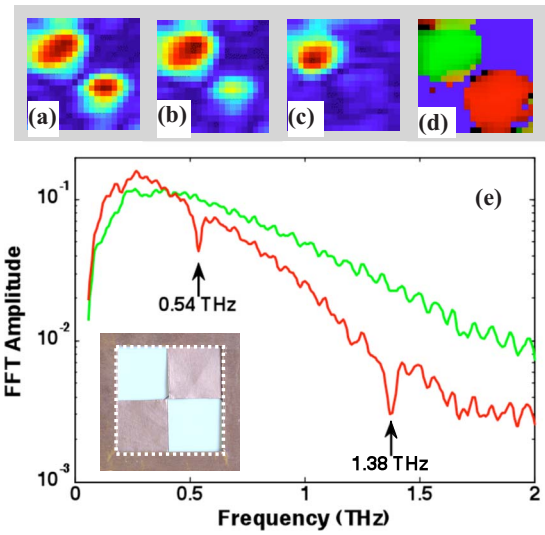

FIG. 2. (Color online) [(a)–(c)] Reconstructed terahertz images of the sample at 0.50, 0.54, and 1.38 THz, respectively. Each image is 40×40 mm^2. (d) RGB chemical map of the sample where red is assigned to lactose, green to polythene, and blue to regions of no transmission (copper areas). (e) Terahertz spectra of polyethylene (upper trace) and lactose (lower trace). The inset shows a photograph of the sample that is made of copper tape with two square holes (each 20×20 mm^2). A 3.0-mm-thick polyethylene pellet is placed at the top-left square while a 3.2-mm-thick lactose pellet is placed at the bottom-right square.

40 THz waveforms were measured; one for each of the 40 masks. Measurements were performed at room temperature with dried air purging to exclude water vapor. In all measurements, the variable delay stage, which provides the time delay between the terahertz pulse and the probe pulse, was scanned over a distance of 5 mm, providing a spectral resolution of 0.03 THz. Each waveform was Fourier transformed into the frequency domain, and the terahertz amplitude at a selected frequency was used for image reconstruction. Two algorithms, the minimum mean square error linear estimation[17] and the TV-min reconstruction algorithm,[10] were used for image reconstruction and the reconstructed images were found to have comparable quality.

Figures 2(a)–2(c) show the terahertz images reconstructed at frequencies of 0.50, 0.54, and 1.38 THz, respectively. At 0.5 THz, the absorption of both polyethylene and lactose is minimal, and this is reflected in the reconstructed image in which two bright regions are observed corresponding to strong terahertz transmission through both materials [Fig. 2(a)]. The dark areas correspond to the opaque copper tape. Lactose monohydrate powder has two well-defined strong absorption features at 0.54 and 1.38 THz.[16] Consequently, at these two frequencies, the reconstructed sample image shows a much weaker transmission for the lactose [bottom-right square of Figs. 2(b) and 2(c)].

A major advantage of terahertz time-domain spectroscopy is that the transient electric field, rather than the radiation intensity, is measured as a function of time. This coherent detection scheme not only yields a terahertz signal with excellent signal-to-noise ratio and high dynamic range, but also preserves the important phase information. This enabled us to measure a terahertz spectrum at each pixel in the image. Figure 2(e) shows the calculated terahertz spectra of the lactose and polyethylene, determined by averaging over an area of 4×4 pixels at the centers of the lactose (top-left square) and polyethylene (bottom-right square) regions. Two well-

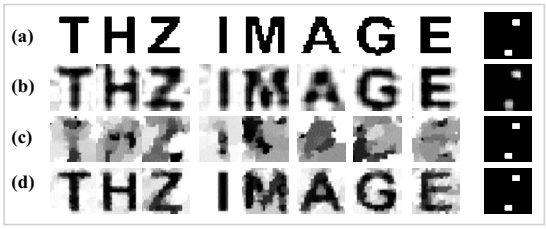

FIG. 3. Simulated results demonstrating the universality of the proposed mask. (a) Original image and reconstructed images using (b) 40 optimized masks, (c) 40 random masks, and (d) 120 random masks.

defined absorption features are observed in the lactose spectrum at 0.54 and 1.38 THz, which agree well with the published data.[18] To the best of our knowledge, this represents the first combined terahertz imaging and spectroscopic measurement using a binary mask set. Furthermore, as a terahertz spectrum was obtained for each pixel of the image, spatially resolved chemical maps of the sample can be obtained by using cosine correlation mapping.[7] For a better visualization of the chemical distributions in the sample, the extracted chemical maps are displayed as a red-green-blue (RGB) map.[7] Figure 2(d) demonstrates that in this way the chemical distribution of the lactose and polyethylene can be clearly distinguished.

It should be emphasized that our mask optimization is based on a general isotropic 2D model, rather than being based on a training set of images. Thus, our masks are generically applicable to a wide range of samples. Indeed, extensive computer simulation demonstrates that our binary approach offers good visual quality for most 20×20 image patches. Figure 3(b) shows one set of such example images obtained using the 40 optimized masks of the test objects shown in Fig. 3(a). In particular, the far-right panel of Fig. 3 shows the image obtained of two light points against a dark background and demonstrates that reasonable image quality is obtained using the mask set in this extreme case. As a comparison, Figs. 3(c) and 3(d) shows images reconstructed using 40 and 120 random masks, respectively. As expected, the optimized masks outperform the random masks at this low sampling rate (10%, i.e., 40 measurements for images comprising 20×20 pixels). The quality of the reconstructed images can be improved by increasing the number of random masks from 40 (a sampling rate of 10%) to, for example, 120 (a sampling rate of 30%), although the measurement time will increase.

In conclusion, we have reported an experimental implementation of terahertz pulsed spectroscopic imaging using an optimized binary mask set. This significantly reduces the number of masks required to form an image, with a commensurate reduction in image acquisition time. Furthermore, we have been able to demonstrate image reconstruction over a far greater frequency range (up to 2 THz), which is of considerable significance for a broad range of imaging applications.

This work was supported by the EPSRC (U.K.) (Grant No. EP/E048811/1). J.A.Z. would like to acknowledge Gonville and Caius College for funding through a research fellowship.

[1] M. Walther, B. Fischer, M. Schall, H. Helm, and P. Uhd Jepsen, Chem. Phys. Lett. **332**, 389 (2000).
[2] Y. C. Shen, P. C. Upadhya, E. H. Linfield, H. E. Beere, and A. G. Davies, Appl. Phys. Lett. **82**, 2350 (2003).
[3] A. G. Davies, A. D. Burnett, W. Fan, E. H. Linfield, and J. E. Cunningham, Mater. Today **11**, 18 (2008).
[4] B. Hu and M. C. Nuss, Opt. Lett. **20**, 1716 (1995).
[5] E. Pickwell, B. E. Cole, A. J. Fitzgerald, M. Pepper, and V. P. Wallace, Phys. Med. Biol. **49**, 1595 (2004).
[6] K. Kawase, Y. Ogawa, Y. Watanabe, and H. Inoue, Opt. Express **11**, 2549 (2003).
[7] Y. C. Shen and P. F. Taday, IEEE J. Sel. Top. Quantum Electron. **14**, 407 (2008).
[8] W. Chan, K. Charan, D. Takhar, K. Kelly, R. Baraniuk, and D. Mittleman, Appl. Phys. Lett. **93**, 121105 (2008).
[9] W. L. Chan, M. L. Moravec, R. G. Baraniuk, and D. M. Mittleman, Opt. Lett. **33**, 974 (2008).
[10] E. Candes, J. Romberg, and T. Tao, IEEE Trans. Inf. Theory **52**, 489 (2006).
[11] W. L. Chan, H. T. Chen, A. J. Taylor, I. Brener, M. J. Cich, and D. M. Mittleman, Appl. Phys. Lett. **94**, 213511 (2009).
[12] Y. C. Shen, P. C. Upadhya, E. H. Linfield, H. E. Beere, and A. G. Davies, Appl. Phys. Lett. **83**, 3117 (2003).
[13] J. Haupt and R. Nowak, *International Conference on Image Processing* (ICIP, Atlanta, 2006), pp. 1269–1272.
[14] Y. Weiss, H.-S. Chang, and W.-T. Freeman, Snowbird Learning Workshop, Allerton, 2007 (unpublished).
[15] N. P. Pitsianis, D. J. Brady, and X. Sun, Proc. SPIE **5817**, 250 (2005).
[16] J. Liang, X. Li, G. Sun, and T. D. Tran, Proceedings of the 2006 IEEE International Conference on Acoustics, Speech, and Signal Processing, Toulouse, France, 2006 (unpublished), Vol. III, pp. 241–244.
[17] S. Haykin, *Adaptive Filter Theory*, 3rd ed. (Prentice-Hall, Englewood Cliffs, 1996).
[18] E. R. Brown, J. E. Bjarnason, A. M. Fedor, and T. M. Korter, Appl. Phys. Lett. **90**, 061908 (2007).